The 2017 World Congress on
Advances in Structural Engineering and Mechanics (ASEM17)
28 August - 1 September, 2017, Ilsan(Seoul), Korea

Time series based damage identification of metro railway structure

Yong-Yi Yan[1)], *Shun Weng[2)], Hong-Ping Zhu[3)] and Kai-Lun Wen[4)]

[1), 2), 3),4)] *School of Civil Engineering and Mechanics, Huazhong University of Science and Technology, Wuhan 430074, China.*
[1)] yyyan@hust.edu.cn
[2)] wengshun@hust.edu.cn
[3)] hpzhu@mail.hust.edu.cn
[4)] kelen_wen@hust.edu.cn

ABSTRACT

Many vibration-based techniques for damage detection have been developed in the past several decades. However most damage detection techniques and validation tests focus on bridge and building structures, but are rarely applied to metro railway structures. Since the finite element model of the metro railway system is very complex, the traditional model-based damage detection and condition assessment are unsuitable. Time series models have been widely used for damage detection due to the sensitivity of the model coefficients and residual errors to the damage in the structure. This paper proposes two kinds of methods for the damage detection of metro railway structure using the Auto-Regressive (AR) model coefficients and residual errors. These methods have been implemented with an experiment conducted on a full-scale two-rings reinforced concrete segmental lining in the laboratory. The results demonstrate that the damage on the segmental lining can be successfully identified and located by these proposed methods.

Keywords: damage identification; time series; metro railway; AR model

1. INTRODUCTION

In the past decades, structural health monitoring have been widely developed due to their promising capacity to provide spatial and quantitative information about structural performance during its whole life cycle. There are two main approaches for structural health monitoring: the model-driven method and data-driven method (Doebling et al. 1998; Cavadas et al. 2013). Model-driven methods establish a high-fidelity physical model of the structure, usually by finite element analysis, and then

---

[1)] Graduate Student
[2)] Associate Professor
[3)] Professor
[4)] Graduate Student

establish a comparison metric between the model and the measured data from the real structure (Weng et al. 2014; Zhu et al. 2015). Data-driven approaches also establish a model, but usually by a statistical representation of the system (Cavadas et al. 2013). The model-based methods is difficult or even impossible to be used to the underground structures, since their finite element model (for example the metro railway system) is very complex.

In search of more reliable damage detection methods, time series models have been widely developed to extract more sensitive damage features since AR model coefficients contain information on structural natural frequencies, model shapes and damping ratios (Nair et al. 2006; Mosavi et al. 2012). AR model coefficients were used as sensitive damage features to detect the damages on a bridge column by Sohn et al. (2000). A simple index computed using the AR model coefficients is applied to detect the damage of a steel beam, and the Fisher information criterion of the computed Damage Sensitive Feature (DSF) is used to statically locate the damage (Jayawardhana et al. 2015). Zheng (2009) used two distance measures of autoregressive (AR) model as damage indicator: one is the Itakura distance and the other is the cepstral distance (Zheng et al. 2009). Nair et al. (2006) has used the first three AR coefficients of the Auto-Regressive Moving Average (ARMA) model. However, it is reported that ARMA models cannot be reliably used to provide spatial information about the detected damages (Pandit & Wu 1983). Lynch et al. (2003, 2004) and Sohn et al. (2001) have used the ratio of standard deviations of the residual errors of the damaged and undamaged Auto Regressive with exogenous input (ARX) models as DSF in their research work. Sohn and Farrar (2001) have found that the ratio of ARX model residual error variances follows the F-distribution, and used hypothesis testing to identify the structural damage. Although many studies on damage identification have been covered in a wide field, few studies have been done on subway lining.

This paper presents two kinds of time-series indices for structural damage detection of metro railway system. The first kind is defined by dealing with the model coefficients, which represents the difference between different damage states of a sensor or the difference two sensors in the same state. The other one takes advantage of the residual errors, which also can be used to describe the difference between different damage states or between two sensors like the former kind. All the methods will be described in detail below. Finally, the proposed methods are applied to identify the damage of an experimental segment lining to investigate its effectiveness.

2. Description of damage detection algorithm

Structural damage has a huge effect on its dynamic properties, which can furtherly change the statistical characteristics of the measured acceleration time histories. Damage detection can be performed using time series analysis of vibration signals measured from a structure before and after damage.

2.1 Background

Before fitting the AR models to the sensor data, it is important to perform standardization (or normalization) in order to compare acceleration time histories (at a sensor location) in different loading conditions (i.e., different magnitudes and directions

of loads) and/or different environmental conditions. After normalization, the features extracted from the signals from undamaged states have similar statistical characteristics to be compared.

Let $x_i(t)$ be the acceleration data from sensor *i*. This sensor data is then partitioned into different streams $x_{ij}(t)$, where *i* denotes the sensor number and *j* denotes the *j*th stream of data from the sensor *i*. The normalized signal $\tilde{x}_{ij}$ is obtained as Eq. (1):

$$\tilde{x}_{ij}(t) = \frac{x_{ij}(t) - \mu_{ij}}{\sigma_{ij}} \tag{1}$$

where μ_{ij} and σ_{ij} are the mean and standard deviation of the *j*th stream of sensor *i*. Hereinafter, $\tilde{x}_{ij}$ will be represented by *y* for notational convenience. Once the initial data pre-processing is completed, the optimal AR model order and its coefficients are estimated for the stationary data. In the AR(*n*) model, the current point in a time series is modeled as a linear combination of the previous *n* points:

$$y(t) = \sum_{j=1}^{n} \phi_j y(t-j) + e(t) \tag{2}$$

where *y*(t) is time history at time *t*, ϕ_j is the undetermined AR coefficient, and e(t) is the residual error with zero mean and constant variance. The values of ϕ_j are estimated by fitting the AR model to the time history data using the Yule-Walker method (Brockwell and Davis 1991). There are several criteria to determine this order. The two most widely used methods are Akaike's information theoretic criterion (AIC) and Akaike's final prediction error (FPE), a detail discussion on AR model order selection can be found in Box et al (2004). In this paper, FPE criterion was used to determine the model order.

2.2 Diagnosis process

Two kinds of methods are proposed to locate the structural damage, the first one uses the model coefficients, and the second one uses the residual errors.

In the first method, the damage sensitive feature named DC is carried out using the model coefficients in each sensor as

$$DC_i = norm(\bar{\phi}_i^u - \bar{\phi}_i^d) \tag{3}$$

where $\bar{\phi}_i^u$ and $\bar{\phi}_i^d$ are the average value of the *i*th sensor's model coefficients in the undamaged state and damaged state, respectively. The *DC* for the *i*th sensor in the undamaged part of the structure will be larger than those in the damaged part, and the *DC* increases with the increase of structural damage.

Furthermore, the relative change of *DC*, namely *DCD,* represents the relative difference of model coefficients between two sensors as

$$DCD_{i,j} = \frac{|norm(\bar{\phi}_i^d - \bar{\phi}_j^d) - norm(\bar{\phi}_i^u - \bar{\phi}_j^u)|}{norm(\bar{\phi}_i^u - \bar{\phi}_j^u)} \tag{4}$$

In the second method, the residual error of AR model is used as damage index. Firstly, a model is built based on the original undamaged structure, and the model. Afterwards, the time series from the damaged state is used to fit the model, and a new set of residual errors is generated. The damage sensitive feature named *DE* is carried out using two kinds of residual errors in each sensor as

$$DE_i = \frac{var(e_i^d)}{var(e_i^u)} \tag{5}$$

where $var(e_i^u)$ and $var(e_i^d)$ respectively represent the variance of *i*th sensor's residual errors in the undamaged and damaged state. The *DE* for the *i*th sensor increases with the increase of structural damage.

In order to identify the location of the structural damage, the relative change of *DE* is defined by

$$DED_{i,j} = \frac{\left|DE_j - DE_i\right|}{DE_i} \tag{6}$$

where the *DED* denotes a relative difference between the sensors *i* and *j*. When the structure is damaged, the *DED* will be very large for two sensors from different states, thus it is useful in damage location.

3. Segmental lining experiment

The subject of the experiment is the full-scale two-rings reinforced concrete segmental lining which is shown in Fig. 1(a).

As shown in Fig. 1(b), the outside diameter of the segmental lining is 4000 mm, the inside diameter is 3500 mm, and the segmental width is 1200 mm per ring. A full ring consists of 6 segments, including a top segment (F segment), two contiguous segments (L1 and L2 segment), and three standard segments (B1, B2 and B3 segment). The corresponding central angle of segment F is 29.0°. The corresponding central angles of L1 and L2 are 53.0°. The corresponding central angles of B1, B2 and B3 are 75.0°. 12 high strength bolts are used to connect the segments in radial direction and 14 high strength bolts are used to connect the two rings in longitudinal direction. The segmental lining is placed on the ground, and there is no constraint between the segmental lining and ground.

Hammer excitation is used in the tests. In the hammer tests, a hammer with the hammerhead weight of 1.5kg was used. A series of 50 hammer hits were recorded in each test configuration. The impact location was on the outside surface of the Ring 1 segmental lining correspond to the measurement point 1(MP1) shown in Fig. 1(a), and the hit was in the direction that perpendicular to the surface of the lining (See Fig. 1(b) for a diagram of the hammer impact locations).

Four DH187E accelerometers with sensitivity of 50mV/g were placed at 4 measurement point (MP1, MP2, MP3 and MP4 in Fig. 2), which were numbered with sensors 1 to 4, to measure the responses of the B2 segment and B3 segment in the direction that perpendicular to the surface of the lining.

A 16-channel DH5922 acquisition system was used to record the structural responses. Antialiasing filters were used in the hammer tests, and the data was sampled at 1000 Hz. The data acquisition system was started prior to the first impact, and a series of 50 hits were recorded within each test configuration.

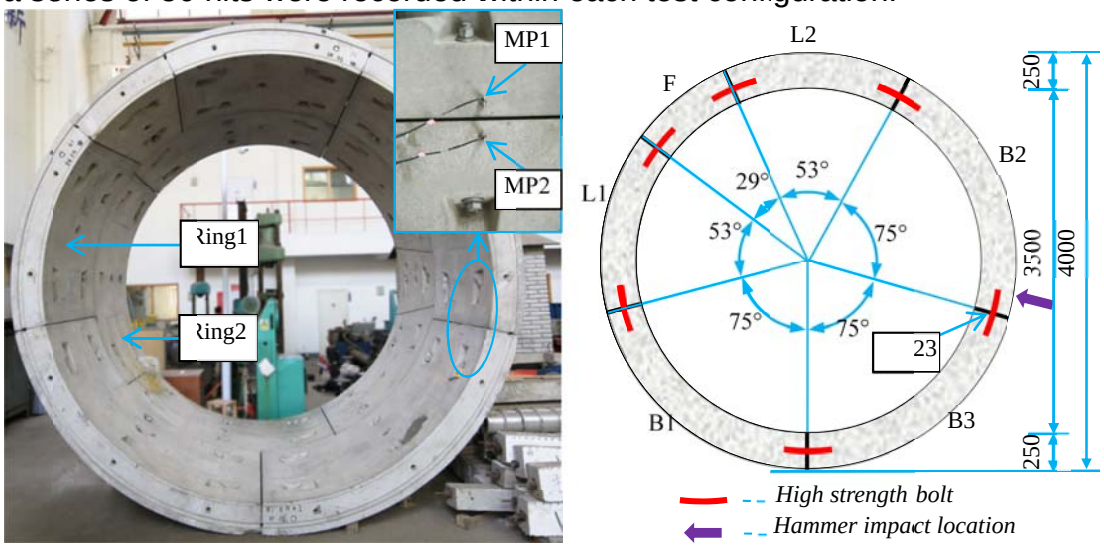

(a) (b)

Fig. 1. Full-scale segmental lining: (a) test site photo; (b) cross section of the Ring 1segmental lining (unit: mm).

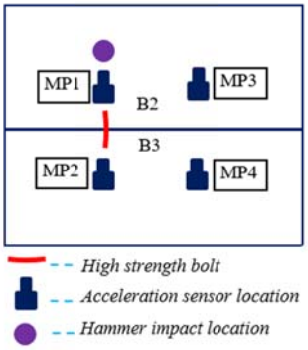

Fig. 2. Sensor location and impact point

Table 1 Description of test cases

Case	Condition	Description
1	Undamaged(U)	Bolt 23 was not loosened
2	Damaged(D1)	Bolt 23 was loosened 180°
3	Damaged(D2)	Bolt 23 was loosened 270°
4	Damaged(D3)	Bolt 23 was removed

A series of tests were conducted on the segmental lining with various damage scenarios. In the tests, damage is simulated by loosening Bolt 23(BL23, see Fig. 1(b)) that connect B2 segment and B3 segment. The various test cases are described in Table 1. It is noted that Cases 2 through 4 are considered as damage scenarios when Case 1 is viewed as the undamaged case. The typical hit acceleration time histories of MP1 and MP2 are shown in Fig. 3.

The order of a time-series model plays an important role in accurate model fitting. Although a high model order will generally reduce the residual error of the model, it is not always advantageous to fit a high order model. This is because, when forecasting using fitted models with high orders, the associated forecasting errors will be higher due to the dependency on errors arising from estimation of the parameters of the model. Thus, obtaining a balance between these two and estimating a reasonable model order are important to increase the accuracy of the results.

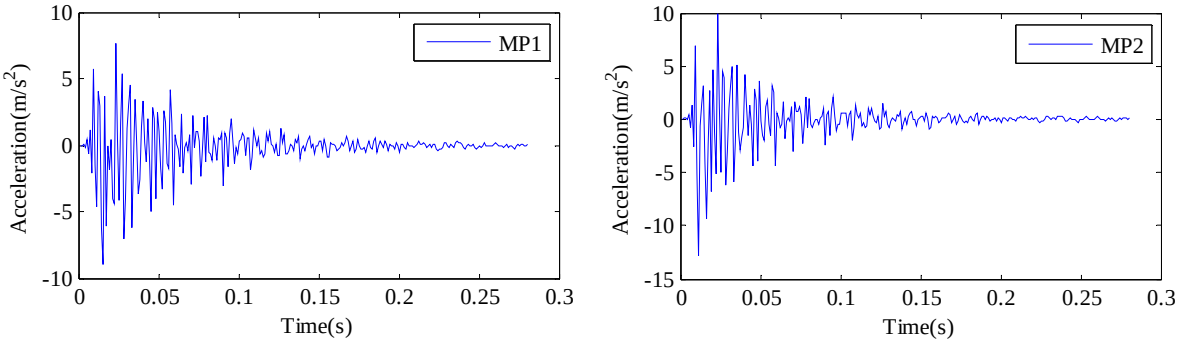

(a) (b)

Fig. 3. Typical hit acceleration time history of MP1 and MP2: (a) MP1; (b) MP2

With the FPE criterion, the optimal model order is the order when FPE criterion is at its minimum, which is given between 35 and 50 in Fig. 4, the optimal model order for the data was selected as 40.

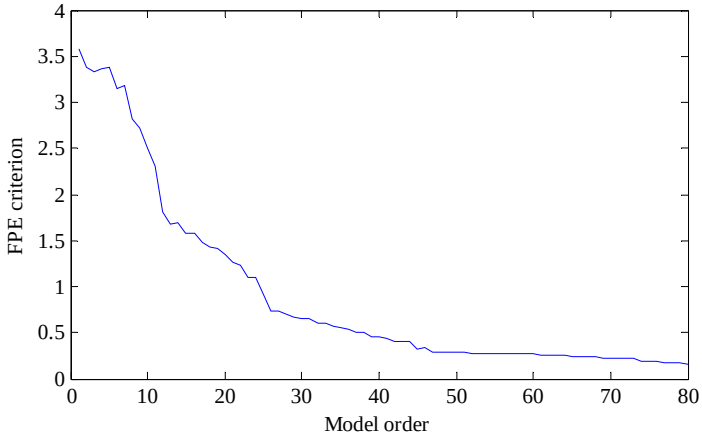

Fig. 4. FPE criterion for model selection

Fig. 5 shows the result of the relative change of model coefficients for the damage cases D2 and D3 in terms of *DC*. It is obvious that the *DC* of sensors 2 and 4 are larger than that of sensors 1 and 3 in Fig. 5(a). This is because, the hammer knocked in the side of sensor 1 and 3, when the bolt 23 was loosened, the impact of the damage in the side of hammer is smaller than that in another side, so the model for sensors 2 and 4 change more obviously than sensor 1 and 3, which influence the model coefficients.

Fig. 5(b) shows a similar result as Fig. 5(a), and the values of *DC* increase with the rise of damage severity. In consequence, *DC* is successfully used for damage detection.

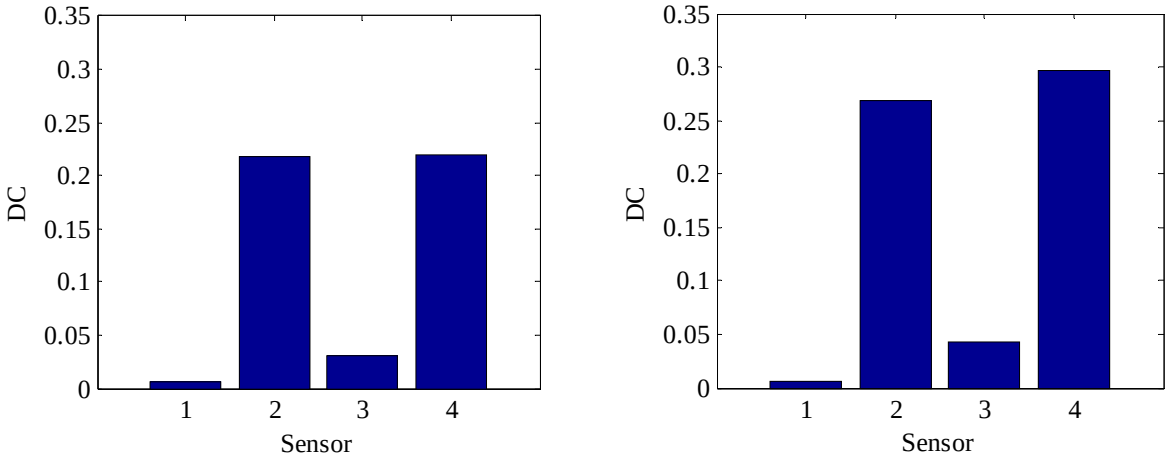

(a) (b)

Fig. 5. Typical *DC* for D2 and D3: (a) D2; (b) D3

In Fig. 6, DCD describes the difference between the sensor pairs by using the model coefficients. The DCD values of sensor pairs 1-2 and 1-4 are greater than the others, which were influenced by the bolt. When the bolt is loosened, the responses of sensors will be different, especially when the sensors come from two segments, which cause the model to vary. But from the figures, the differences between sensor pairs 2-3 and 2-4 cannot be found. The values of sensors from one segment will be very small for example sensors 1-3 and 2-4. Comparing Fig. 6(a) and Fig. 6(b), it is evident that the values grow with the rise of damage severity. DCD successfully identifies the damage location as well.

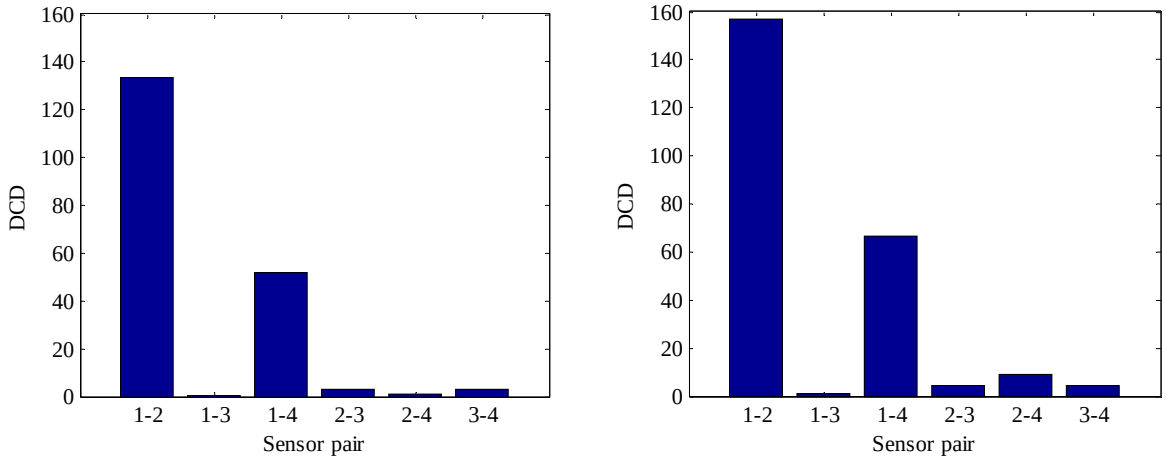

(a) (b)

Fig. 6. Typical *DCD* for D2 and D3: (a) D2; (b) D3

In addition, the residual errors are used to identify the damage in terms of *DE*. Fig.7(a) and Fig.7(b) show that the DE increases with the increase of damage severity. *DE* is 1 when the structure is undamaged, and it will be larger in the damaged state. The model for this method is built in the undamaged state, and it is more suitable to the undamaged series than the damaged series. When the damaged series fit to the undamaged model, the residual errors will be larger than those from undamaged state.

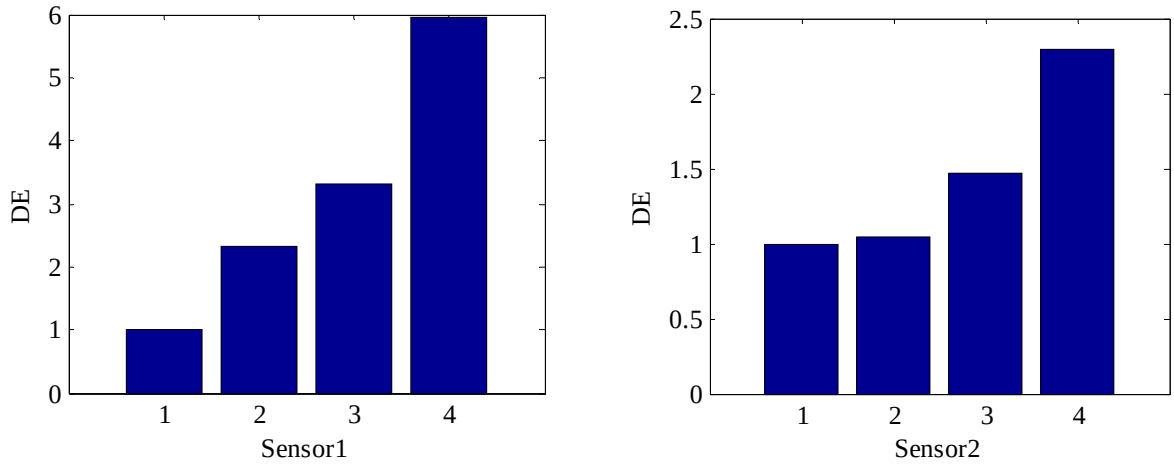

(a) (b)

Fig. 7. *DE* of sensor 1 and 2: (a) sensor1; (b) sensor2

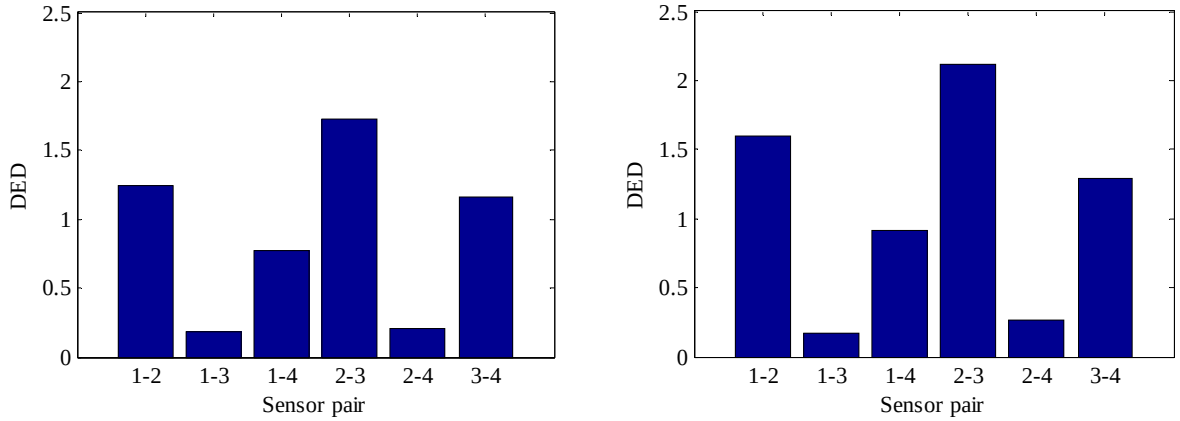

(a) (b)

Fig. 8. *DED* for different damages: (a) D2; (b) D3

In order to locate the damage, the *DED* was calculated based on the *DE*, with the result shown in Fig.8. It is obvious that the *DED* of sensor pairs 1-2, 1-4, 2-3, and 3-4 are larger than the others in Fig. 8(a), the reason is that those sensor pairs consist of sensors from two different segments of the segmental lining, when the bolt is loosened, the damage will influence the relation between sensors in damaged part and undamaged part. So the *DED* can locate the damage. Comparing those two pictures in Fig.8, it is obvious that the *DED* increases with the risk of damage severity.

4. CONCLUSIONS

This paper proposed two kinds of methods to identify and locate the damage based on the model coefficients and the residual errors of AR model, the *DC* and *DCD* take advantage of the model coefficients, and the *DE* and *DED* make use of the residual errors. These methods were verified by a full-scale reinforced concrete segmental lining. The results show that all these damage sensitive features are successful in detecting damage location accurately, and the value of these features increase with the rise of damage severity.

REFERENCES

Brockwell, P.J. and David, R.A. (1991), *Time series: Theory and methods*, Springer, New York, US.

Box, G.E.P., Jenkins, G.M. and Reinsel, G.C. (1994), *Time Series Analysis: Forecasting and Control*, Prentice-Hall, Englewood Cliffs, N.J.

Cavadas, F., Smith, I.F.C. and Figueiras, J. (2013), "Damage detection using data-driven methods applied to moving-load responses", *Mech. Syst. Signal Pr.*, **39**(1-2), 409-425.

Doebling, S.W., Farrar, C.R. and Prime, M.B. (1998), "A summary review of vibration-based damage identification methods", *Shock Vib.* Digest, **30**(2), 91-105.

Jayawardhana, M., Zhu, X.Q., Liyanapathirana, R. and Gunawardana, U. (2015), "Statistical damage sensitive feature for structural damage detection using AR model cpefficients", *Adv. Struct. Eng.*, **18**(10), 1551-1562.

Lynch, J.P., Sundararajan, A., Law, K.H., Kiremidjian, A.S. and Carryer, E. (2004), "Embedding damage detection algorithms in a wireless sensing unit for operational power efficiency", *Smart Mater. Struct.*, **13**(4), 800-810.

Lynch, J.P., Sundararajan, A., Law, K.H., Kiremidjian, A.S., Kenny, T. and Carryer, E. (2003), "Embedment of structural monitoring algorithms in a wireless sensing unit", *Struct. Eng. Mech.*, **15**(3), 285-297.

Mosavi, A., Dickey, D., Seracino, R. and Rizkalla, S. (2012), "Identifying damage locations under ambient vibrations utilizing vector autoregressive models and Mahalanobis distance". *Mech. Syst. Signal Pr.*, **26**(1), 254-267

Nair, K.K., Kiremidjian, A.S. and Law, K.H. (2006), "Time series based damage detection and localization algorithm with application to the ASCE benchmark structure", *J. Sound Vib.*, **291**(1-2), 349-368.

Pandit, S.M. and Wu, S.M. (1983), *Time Series and System Analysis with Applications*, Wiley, New York, US.

Sohn, H., Czarnecki, J.A. and Farrar, C.R. (2000), "Structure health monitoring using statistical process control", *J. Struct. Eng.*, **126**(11), 1356-1363.

Sohn, H. and Farrar, C.R. (2001), "Damage diagnosis using time series analysis of vibration signals", *Smart Mater. Struct.*, **10**(3), 446-451.

Sohn, H., Farrar, C.R., Hunter, N.F. and Worden, K. (2001), "Structural health monitoring using statistical pattern recognition techniques", *J. Dyn. Syst-T. Asme*, **123**(4), 706-711.

Weng, S., Zhu, A.Z., Zhu, H.P., Xia, Y. and Mao, L. (2014), "Dynamic condensation approach to the calculation of eigensensitivity", *Comput. Struct.*, **132**, 55-64.

Zhu, H.P., Mao, L., and Weng, S. (2014), “A sensitivity-based structural damage identification method with unknown input excitation using transmissibility concept”, *J. Sound. Vib.*, **333**(26), 7135-7150.

Zheng, H.T. and Mita, A. (2009), “Localized damage detection of structures subject to multiple ambient excitations using two distance measures for autoregressive models”, *Struct. Health Monit.*, **8**(3), 207-216.